Available online at www.sciencedirect.com
ScienceDirect
Trans. Nonferrous Met. Soc. China 27(2017) 578−583

Transactions of
Nonferrous Metals
Society of China
www.tnmsc.cn

Synthesis of biomorphic hierarchical CeO_2 microtube with enhanced catalytic activity

Jing-jing HUANG[1], Chen-cheng WANG[1], Lu-tian JIN[1], Feng CHEN[1,2], Zhi-gang CHEN[1,2]

1. School of Chemistry, Biology and Materials Engineering,
Suzhou University of Science and Technology, Suzhou 215009, China;
2. Jiangsu Key Laboratory for Environment Functional Materials,
Suzhou University of Science and Technology, Suzhou 215009, China

Received 12 January 2016; accepted 19 May 2016

Abstract: A biomorphic CeO_2 microtube with multiple-pore structure was fabricated by using the cotton as biotemplate, through cerium nitrate solution infiltration and thermal decomposition. Field emission scanning electron microscope (FESEM), powder X-ray diffraction (XRD), transmission electron microscope (TEM), N_2 adsorption−desorption isotherms, temperature-programmed reduction (TPR) and CO oxidation were used to characterize the samples. The results indicated that the synthesized products were composed of crystallites with grain size about 9 nm and exhibited a fibrous morphology similar to the original template and possessed a specific surface area (BET) of 62.3 m^2/g. Compared with the conventional CeO_2 particles, the synthesized materials showed a superior catalytic activity for CO oxidation. For the synthesized fibrous CeO_2, the CO conversion at 320 °C was above 90% and a 100% CO conversion was obtained at 410 °C.

Key words: synthesis; biotemplate; multiple-pore structure; ceria; catalytic performance

---

1 Introduction

Recently, artificial morphology-controlled materials have attracted considerable attention due to their outstanding physical and chemical properties [1−3]. Various approaches have been reported to fabricate complex hierarchical structure including atomic layer deposition [4], hydrothermal treatment [5] and biotemplate synthesis [6]. Among these methods, biomorphic templating has been noteworthy as an available technique to fabricate inorganic materials with predetermined microstructures, owing to its low cost and simple process. Up to now, a serious of novel biomorphic metal oxides with large specific surface area and hierarchical structure have been developed by using biotemplates, such as protein [7], virus particles [8], diatom [9], yeast [10], and butterfly wings [11]. PENG et al [12] introduced a novel biosorbent prepared by loading saccharomyces cerevisiae onto nano-Fe_3O_4. The biomorphic ceria materials have been prepared using bamboo leaves as template [13].

CeO_2, as one of the most important rare earth oxides, has been extensively studied and widespread applied in catalysis [14], gas sensing [15] and solar cell [16]. ZHANG et al [17] reported the controlled synthesis and special properties of ceria nanorods. Most recently, the morphology dependence of catalytic properties of Ni/CeO_2 nanostructures has been reported for carbon dioxide reforming to methane [18], ketone [19], and bio-ethanol [20]. Functional materials with hierarchical structure could provide higher specific surface area and better properties than their bulk countparts, which can be used to develop new potential applications. Although numerous efforts have been directed to the synthesis of hierarchical microtube, few researches have been

---

Foundation item: Projects (21277094, 51478285, 21407111) supported by the National Natural Science Foundation of China; Projects (BK20140280, BK20151198) supported by the Natural Science Foundation of Jiangsu Province, China; Project (14KJA430004) supported by Collegiate Natural Science Fund of Jiangsu Province, China; Project supported by the Priority Academic Program Development of Jiangsu Higher Education Institutions (PAPD), China; Project supported by Jiangsu Collaborative Innovation Center of Technology and Material for Water Treatment, China; Project supported Excellent Innovation Team in Science and Technology of Education Department of Jiangsu Province, China; Projects (SJHG1304, SJHG1310, SJHG1404) supported by the Jiangsu Key Laboratory for Environment Functional Materials, China

Corresponding author: Zhi-gang CHEN; Tel: +86-13906207666; E-mail: czg@ujs.edu.cn

DOI: 10.1016/S1003-6326(17)60064-5

concerned with ceria material.

We chose the plentiful agricultural product, cotton, as the biotemplate to fabricate hierarchical CeO_2 microtube. The diverse hierarchy of natural cotton has been faithfully replicated from nanometer scale by CeO_2 nanoparticle to the microscopic scale by CeO_2 microtube. This novel synthesis method can serve as a guideline to fabricate other hierarchical inorganic materials.

2 Experimental

2.1 Sample preparation

All the reagents were purchased from Sinopharm Chemical Reagent Co., Ltd. They were of analytical grade and used without further purification. The absorbent cotton as template was commercially available. The templates were impregnated with 0.1 mol/L cerium nitrate ($Ce(NO_3)_3\cdot 6H_2O$) solution (RT, 72 h), dried in air (80 °C for 1 h), and finally calcined in air to 550 °C at a heating rate of 2 °C/min to burn away biotemplates and yield biomorphic ceria product. For comparison, nontemplated ceria was prepared through the same procedures without pledget.

2.2 Characterization

The changes in mass of the samples during calcinations were measured using a thermogravi-metric analyzer (TGA, TG 209 F3, Netzsch). The crystalline phases in the products were identified by using diffraction analysis (XRD, with Cu K_α radiation source, Rigaku D/max 2500 PC, Japan) operated at 40 kV. Field emission scanning electron microscopy (FESEM, Hitachi S4800, Japan) was used to characterize the morphology of the samples. Transmission electron microscopy (TEM) measurements were performed on a JEM−2100 with a Gatan CCD camera. Specific surface area and pore-size distribution were derived from nitrogen adsorption−desorption isotherms obtained at −196 °C on an Autosorb-iQ2-MP apparatus. Temperature-programmed reduction (TPR) analysis was conducted on a TP−5000 analyzer with a TCD detector (Tianjin, China). The TPR profile of the powder (about 50 mg) was recorded between 20 °C and 780 °C at a heating rate of 10 °C/min under 10% hydrogen in nitrogen.

2.3 catalytic test of CO oxidation

The catalytic tests were conducted in a temperature-programmed reaction system equipped with a mass chromatography (GC 950 system, Shanghai Haixin, China) for product analysis in a typical reaction, 100 mg product was loaded in a quartz reactor and heated from room temperature to 500 °C at a heating rate of 5 °C/min. The gas flow of 50 mL/min was composed of 5% O_2 and 1% CO with N_2 as balance.

3 Results and discussion

3.1 TG−DTA analysis

The burning process was recorded to identify the calcination temperature of the cotton and cerium nitrate precursor composite by TG−DTA analysis. The corresponding curves are shown in Fig. 1. Three stages can be identified in the thermal decomposition. A small scale mass loss of the composite at about 100 °C was mainly due to the removal of physisorbed water, which is confirmed in the corresponding DSC data, where a small scale of endotherm was observed [21]. The subsequent rapid mass loss (about 73%) occurring at 349 °C was attributed to the charring of the scape template and the transformation of the precursor. In this stage, a lot of O_2, CO, CO_2, etc. were released, which could promote the further decomposition of the composite. The observed exothermic peak centered at 494 °C can be ascribed to the further decomposition of the cellulose and crystallization of the precursor. Finally, there was no mass loss after the temperature reached 530 °C, indicating that all the scape templates were removed and the stable CeO_2 crystal was formed [22]. Therefore, the synthesizing temperature of the replicas can be identified as 550 °C based on the analysis.

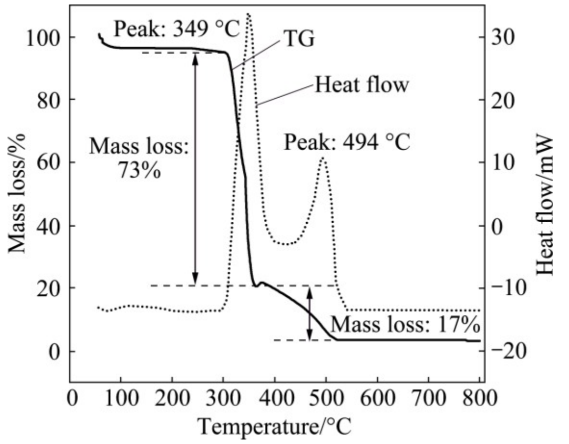

Fig. 1 TG−DTA analysis of thermal decomposition of scape after being impregnated with cerium nitrate

3.2 FESEM images of biomorphic ceria

Figure 2 shows FESEM images of the synthesized CeO_2 derived from scape template after being calcined at 550 °C in air. As can be seen from the images, the replicas mimicked the shape of the scape template perfectly and exhibited a fibrous microstructure. The randomly arranged fibrous structure of the samples was 3−8 μm in diameter, with lengths ranging from 60 to 200 μm. Fibers which displayed a warped edge can be ascribed to the shrink during the calcination process

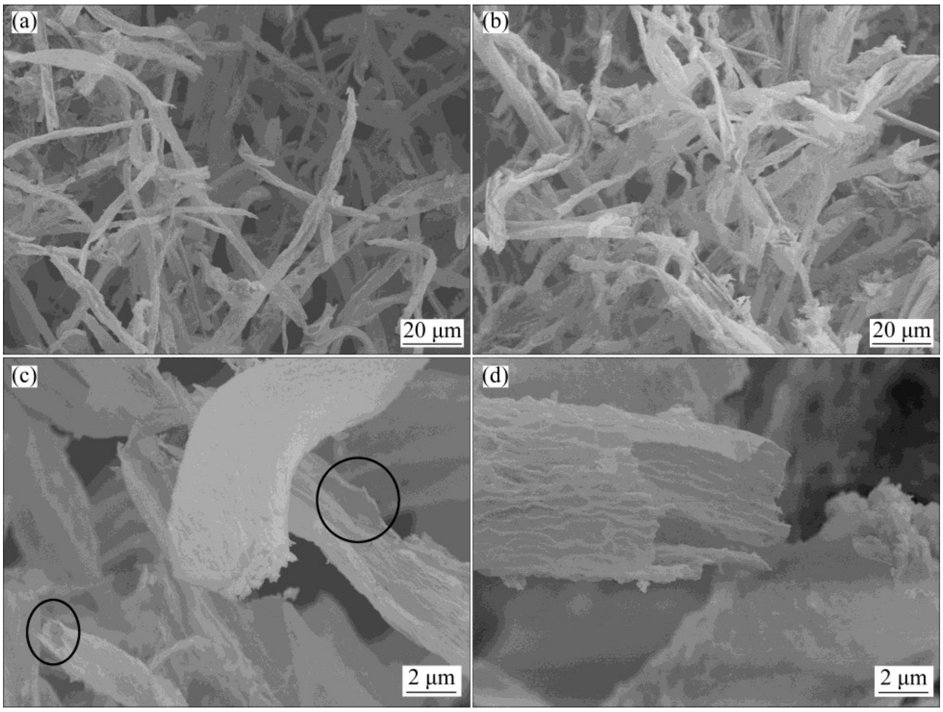

Fig. 2 FESEM images of biomorphic CeO_2-templated from scape, showing fibre-like and hollow tubular (black oval) assemblies: (a, b) Lower magnification; (c, d) Higher magnification

(Figs. 2(a) and (b)). This crimped edge has formed hollow tubular structure (see Fig. 2(c)). A broken end of one microfiber can be clearly observed, showing the hollow structure with an inner diameter of 4 μm. It is worth noting that the micro-sized hollow fibre is overlaid with ridges. This hollow structure with ridges can largely increase the specific surface area of the biomorphic ceria, and further improve its catalytic performance (Fig. 2(d)).

3.3 TEM images and XRD pattern

Further information of the biomorphs is provided by TEM and the corresponding HETEM images. The vast cell structure of the resulting products in Fig. 3(a) demonstrated that the replica retained the microstructure of original scape templates. The cell size is about 100 nm, as can be seen in Fig. 3(b). Moreover, irregular ceria polycrystals with grain size arranged from 6 to 15 nm were composed of the microtube. HRTEM images in Figs. 3(c)−(e) revealed that the fibrous structure comprised CeO_2 nanocrystals with diameters of approximately 9 nm. The SAED pattern, shown in the inset of Fig. 3(c), confirmed that the calcined product was composed of CeO_2 nanopaticles with a polycrystalline structure. The most important is that a number of pores (marked with white square in Fig. 3(c)) with different sizes exist in the resulting material. The formation of these mesopores is attributed to the overflow of gas generated during the scape templates removing procedure. These porous materials are believed to be more active catalysts in comparison with their bulk countparts owing to the easy accessibility of the guest molecules to active sites in the complex framework [23].

The XRD pattern of the samples templated from the scape is shown in Fig. 3(f). All of the peaks can be assigned to cubic fluorite CeO_2, which are in good agreement with the reported data (PDF No. 0180), without crystalline impurities. The crystallite size has been estimated to be 9 nm by using the Scherrer formula. This result is in good agreement with HRTEM analysis.

3.4 N_2 adsorption−desorption isotherms

Typical N_2 adsorption−desorption isotherm and the corresponding pore size distribution of the porous ceria fibers are presented in Fig. 4. This isotherm of porous CeO_2 exhibits a IV-type isotherm [24], typical of mesoporous materials with a step at relative pressure of 0.4−1.0 (p/p_0), and H3-type hysteresis loop owing to capillary condensation. The sharp step occurring in the high relative pressure range of 0.9−1.0 indicated that the CeO_2 fibers also possessed some macroporous structures [25]. On the basis of BET equation, the specific surface area of the porous ceria fiber is 62.3 m^2/g. The corresponding BJH pore size distribution curve shows a multi-pore diameter distribution within the range of a mesopore (2−50 nm), which is in accordance with the previous HRTEM observation. These porous structures further increased the specific surface area of the resulting products, therefore, an enhanced catalytic properties was obtained.

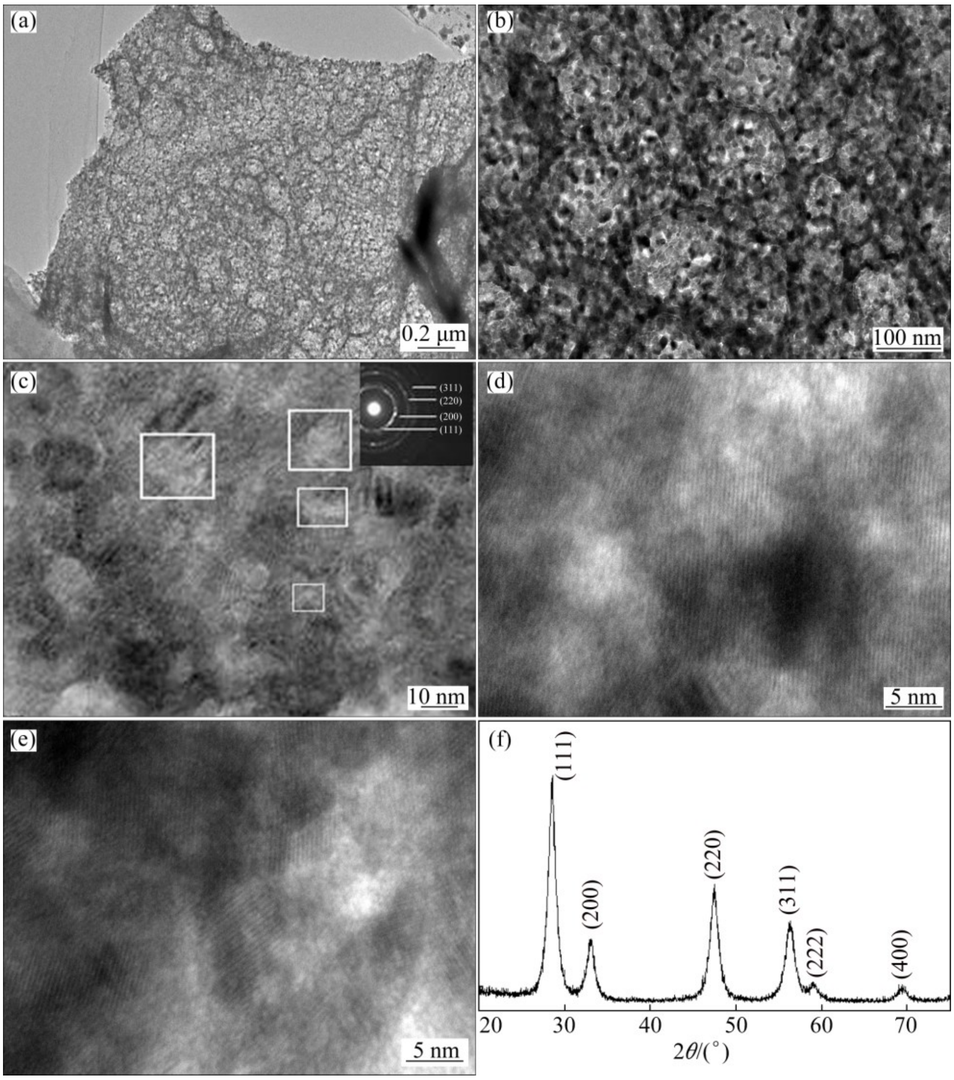

Fig. 3 TEM images (a−e) and XRD pattern (f) of CeO_2 fibers synthesized by using scape as template

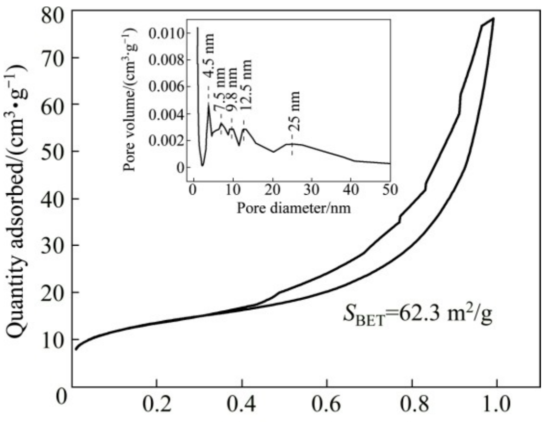

Fig. 4 N_2 adsorption−desorption isotherm and corresponding pore size distribution curve of porous CeO_2 replicas

3.5 Temperature-programmed reduction (TPR) analysis

H_2-TPR has been widely used to characterize the catalytic properties of catalysts. For comparison, pure CeO_2 (BET specific surface area of 6.7 m^2/g) was synthesized by calcinating cerium nitrate to 550 °C. The results obtained by temperature-programmed reduction of the samples are illustrated in Fig. 5. Ceria materials display a bimodal peak, divided into surface and bulk oxygen reduction, respectively [26,27]. The bulk CeO_2 displayed two peaks at about 520 and 740 °C, while the biomorphic CeO_2 showed the peaks at about 520 and 670 °C. The relative peak intensity at 740 °C in pure CeO_2 demonstrates that bulk oxygen reduction is the main process (Fig. 5(a)). The sharp peak of biomorphic CeO_2 centered at 520 °C shows surface oxygen reduction as the main reduction process, indicating an enhanced surface oxygen activity of synthesized samples. Surface oxygen is the active species and is found to account for high performances of ceria materials [28]. On one hand, the fibrillar structure and porous feature of the resulting product increased its specific surface area to provide more active sites for reduction [29], on the other hand, the porous structure facilitates mass transfer to promote the chemical activity of the synthesized materials. It can also be seen in Fig. 5 that the high-temperature peak of biomorphic sample shifts to a lower temperature range from 744 to 670 °C further proved by the superior mass transfer and an higher surface area of the porous CeO_2 replicas.

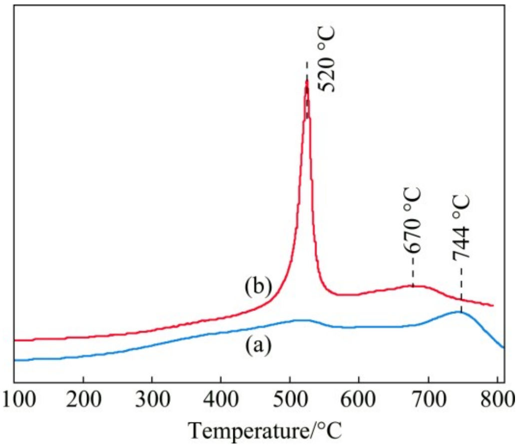

Fig. 5 H_2-TPR profiles: (a) Bulk CeO_2; (b) Porous CeO_2 fiber

3.6 CO oxidation test

Figure 6 shows the catalytic performance for CO oxidation over the CeO_2 fibers and a reference bulk CeO_2 sample synthesized without a template. Clearly, the CO conversion increased with increasing reaction temperature for both samples. The CO conversion of the bulk products at about 320 °C was above 20%. Compared with the bulk products, the CO conversion of synthesized fibrous CeO_2 at about 320 °C was above 90% and 100% CO conversion was achieved at 410 °C. The T_{50} of the biomorph replica was 235 °C, while it was about 435 °C for the bulk CeO_2, indicating a great enhancement in catalytic performance of the resulting CeO_2 fibers. Besides the increased specific surface areas, the porous structure is also believed to provide sufficient space for the adsorption of O_2 gas molecular. Therefore, the obtained CeO_2 fibers show superior catalytic performance compared with the conventional bulk ones.

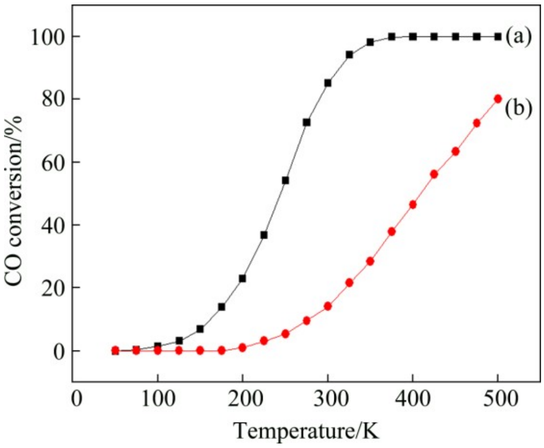

Fig. 6 Catalytic activity of porous CeO_2 fibers templated from scape (a) and bulk CeO_2 (b)

4 Conclusions

1) A CeO_2 fiber with multiple-pore structures was synthesized by using the scape of cotton as a biotemplate. This fibrous structure of products, consisting of crystallites with grain size about 9 nm was 3−8 μm in diameter, with lengths ranging from 60 to 200 μm.

2) The synthesized materials showed an enhanced surface oxygen activity, as was discussed in detail by TPR analysis. The results obtained by temperature-programmed reduction of the samples are illustrated, the fibrillar structure and porous feature of the resulting product increased its specific surface areas to provide more active sites for reduction. Moreover, the porous structure facilitates mass transfer to promote the chemical activity of the synthesized materials.

3) The products also displayed a superior catalytic activity for CO oxidation. For the synthesized fibrous CeO_2, the CO conversion at 320 °C was above 90% and 100% CO conversion was obtained at 410 °C, suggesting its potential in catalysis, sensing, auto-gas purification, etc.

References

[1] ZHANG Yan-hua, LIU Xiao-yan, HUANG Jian-guo. Hierarchical mesoporous silica nanotubes derived from natural cellulose substance [J]. Appl Mater Interfaces, 2011, 3: 3272−3275.

[2] ALLOYEAU D, STEPHANIDIS D, ZHAO X. Biotemplated synthesis of metallic nanoclusters organized in tunable two-dimensional superlattices [J]. J Phys Chem C, 2011, 115: 20926−20930.

[3] ZHAO Yu-fei, WEI Min, LU Jun. Biotemplated hierarchical nanostructure of layered double hydroxides with improved photocatalysis performance [J]. ACS Nano, 2009, 3: 4009−4016.

[4] KNEZ M, KADRI A, WEGE C. Atomic layer deposition on biological macromolecules: Metal oxide coating of tobacco mosaic virus and ferritin [J]. Nano Letters, 2006, 6: 1172−1177.

[5] NURAGE N, DANG X N, QI J F. Biotemplated synthesis of perovskite nanomaterials for solar energy conversion [J]. Adv Mater, 2012, 24: 2885−2889.

[6] WANG Shu-rong, ZHANG Jun, JIANG Jun-qing. Porous ceria hollow micro-spheres: Synthesis and characterization [J]. Microporous Mesoporous Mater, 2009, 123: 349−353.

[7] CHEN Yu-lin, GUAN Zhi-bin. Bioinspired modular synthesis of elastin-mimic polymers to probe the mechanism of elastin elasticity [J]. J Am Chem Soc, 2010, 132: 4577−4579.

[8] SINGH S, BHATTA U M, SATYAM P V. Bacterial synthesis of silicon/silica nanocomposites [J]. J Mater Chem, 2008, 18: 2601−2606.

[9] PEREZ-CABER M P C, PUCHOL V, BELTRAN D. Thalassiosira pseudonana diatom as biotemplate to produce a macroporous ordered carbon-rich material [J]. Carbon, 2008, 46: 297−304.

[10] BAI Bo, WANG Peng-peng, WU Le. A novel yeast bio-template route to synthesize Cr_2O_3 hollow microspheres [J]. Mater Chem Phys, 2009, 114: 26−29.

[11] PENG Wen-hong, ZHU Shen-min, WANG Wan-lin. 3D network magnetophotonic crystals fabricated on morpho butterfly wing templates [J]. Adv Funct Mater, 2012, 22: 2072−2080.

[12] PENG Guo-wen, DING De-xin, HU Nan, YANG Yu-shan, WANG Xiao-liang. Adsorption properties and mechanism of saccharomyces cerevisiae loaded by nano-Fe_3O_4 on uranium [J]. The Chinese Journal of Nonferrous Metals, 2012, 22(2): 604−610. (in Chinese)

[13] WANG Wei, CHEN Zhi-gang, CHEN Feng, WANG Tai-bin. Synthesis of hierarchical porous ceria templated from bamboo leaves and their catalytic performance [J]. The Chinese Journal of Nonferrous Metals, 2012, 22(9): 2565−2571. (in Chinese)

[14] LI Yuan-zhi, SUN Qian, KONG Ming. Coupling oxygen ion conduction to photocatalysis in mesoporous nanorod-like ceria significantly improves photocatalytic efficiency [J]. J Phys Chem C, 2011, 115: 14050−14057.

[15] LU Z S, KULLGREN J, YANG Z X. Sulfidation of ceria surfaces from sulfur and sulfur diffusion [J]. J Phys Chem C, 2012, 116: 8417−8425.

[16] KUBACKA A, MARCOS F G, GERARDO C. Advanced nanoarchitectures for solar photocatalytic applications [J]. Chem Rev, 2012, 112: 1555−1614.

[17] ZHANG Deng-song, DU Xian-jun, SHI Li-yi, GAO Rui-hua. Shape-controlled synthesis and catalytic application of ceria nanomaterials [J]. Dalton Trans, 2012, 41: 14455−14475.

[18] DU Xian-jun, ZHANG Deng-song, SHI Li-yi, GAO Rui-hua, ZHANG Jian-ping. Morphology dependence of catalytic properties of Ni/CeO_2 nanostructures for carbon dioxide reforming of methane [J]. J Phys Chem C, 2012, 116: 10009−10016.

[19] PENDYALA V R R, VANAMA P K, GINJUPALLI S R. Vapor phase selective hydrogenation of acetone to methylisobutyl ketone (MIBK) over Ni/CeO_2 catalysts [J]. Catal Sci Technol, 2012, 2: 1665−1673.

[20] FRUSTERI F, FRENI S, CHIODO V. Steam and auto-thermal reforming of bio-ethanol over MgO and CeO_2/Ni supported catalysts [J]. Int J Hydrogen Energy, 2006, 31: 2193−2199.

[21] LIU Xiao-yan, GU Yuan-qing, HUANG Jian-guo. Hierarchical, titania-coated, carbon nanofibrous material derived from a natural cellulosic substance [J]. Chem Eur J, 2010, 16: 7730−7740.

[22] GUI Zhan-kui, LIU Jun, ZENG Da-wen. Quasi-one-dimensional bismuth tungsten oxide nanostructures templated by cotton fibers [J]. J Am Ceram Soc, 2010, 5: 1479−1483.

[23] HU Chao-quan, ZHU Qing-shan, JIANG Zheng. Preparation and formation mechanism of mesoporous CuO−CeO_2 mixed oxides with excellent catalytic performance for removal of VOCs [J]. Microporous Mesoporous Mater, 2008, 113: 427−434.

[24] LEVENTIS N, SADEKAR A, NAVEEN, CHANDRASEKARAN. Click synthesis of monolithic silicon carbide aerogels from polyacrylonitrile-coated 3D silica networks [J]. Chem Mater, 2010, 22: 2790−2803.

[25] ZHANG Yan-hua, LIU Xiao-yan, HUANG Jian-guo. Hierarchical mesoporous silica nanotubes derived from natural cellulose substance [J]. Appl Mater Interfaces, 2011, 3: 3272−3275.

[26] REN Yu, BRUCE P G, MA Zhen. Solid−solid conversion of ordered crystalline mesoporous metal oxides under reducing atmosphere [J]. J Mater Chem, 2011, 21: 9312−9318.

[27] RUMRUANGWONG M, WONGKASEMJI S. Synthesis of ceria–zirconia mixed oxide from cerium and zirconium glycolates via sol–gel process and its reduction property [J]. Appl Organometal Chem, 2006, 20: 615−625.

[28] LIU Xiang-wen, ZHOU Ke-bin, WANG Lei. Oxygen vacancy clusters promoting reducibility and activity of ceria nanorods [J]. J Am Chem Soc, 2009, 131: 3140−3141.

[29] BRUCE L, HOANG M, HUGHES A. Surface area control during the synthesis and reduction of high area ceria catalyst supports [J]. Appl Catal A, 1996, 134: 351−362.

生物形态的层次 CeO_2 微管的合成及其催化活性的增强

黄晶晶 [1]，王陈程 [1]，金璐甜 [1]，陈 丰 [1,2]，陈志刚 [1,2]

1. 苏州科技学院 材料化学与生物工程学院，苏州 215009；
2. 苏州科技学院 江苏省环境功能材料重点实验室，苏州 215009

摘 要：以棉花为模板、经硝酸铈溶液浸渍后煅烧，合成多孔结构的生物形态二氧化铈微管材料。采用场发射扫描电子显微镜(FESEM)、X 射线衍射(XRD)、透射电子显微镜(TEM)、N_2 吸脱附程序升温还原(TPR)和 CO 氧化等手段对样品进行表征。结果表明，合成的材料是由尺寸约 9 nm 的晶粒组成，复制出原模板的纤维形貌，比表面积(BET)为 62.3 m^2/g。与传统 CeO_2 微粒相比，在 CO 氧化实验中，所合成的材料表现出极高的催化活性。所合成的纤维状 CeO_2 在 320 °C 下 CO 的转化率约为 90%，在 410 °C 下 CO 的转化率达到 100%。

关键词：合成；生物模板；多孔结构；氧化铈；催化性能

(Edited by Wei-ping CHEN)